Reaction kinetic behavior of sulfated-zirconia catalysts for butane isomerization

Z. Hong, K.B. Fogash[1], J.A. Dumesic[*]

Department of Chemical Engineering, University of Wisconsin, Madison, WI 53706, USA

Abstract

Sulfated-zirconia catalysts show rapid deactivation (deactivation constants near $0.02 \, min^{-1}$) during isomerization of *n*-butane when olefins are present in the feed. Removal of olefins from the feed decreases the rate of catalyst deactivation over sulfated-zirconia (to values near $0.007 \, min^{-1}$). The rates of deactivation are slower during isobutane isomerization (deactivation constants near $0.003 \, min^{-1}$) than during *n*-butane isomerization over sulfated-zirconia catalysts in the presence of feed olefins. Deactivation of the catalysts during *n*-butane isomerization appears to be caused by the production of coke on the catalyst from straight-chain olefinic species either present in the feed or produced on the catalyst under reaction conditions. Butane isomerization over sulfated-zirconia can be viewed as being a surface chain reaction comprising initiation, propagation, and termination steps. The primary initiation step in the absence of feed olefins is the dehydrogenation of butane over sulfated-zirconia, generating butenes which adsorb onto acid sites. Quantum-chemical calculations, employing density functional theory, suggest that the dissociative adsorption of dihydrogen, isobutylene hydrogenation, and dissociative adsorption of isobutane are feasible over the sulfated-zirconia cluster, and these reactions take place over the Zr–O sites. © 1999 Elsevier Science B.V. All rights reserved.

Keywords: Sulfated-zirconia; Solid acid catalysts; Isomerization; Butane; Deactivation; Microcalorimetry; Selective poisoning; Surface chain reaction; Density functional theory

1. Introduction

The effective utilization of chemical feedstocks is of paramount importance for economic and environmental reasons. For example, the viability of a chemical process may depend on achieving a specific yield or selectivity for particular products in this age of increasing commercial competitiveness. Furthermore, the application of a chemical process may be determined by the impact of this process on the environment. Thus, it is necessary to identify processes that achieve high yields of desired products while inhibiting the formation of undesirable by-products. In this respect, sulfated metal oxides have attracted considerable interest because they are more environmentally benign, and more active and selective for the transformation of hydrocarbons at low temperatures than the current systems [1]. In particular, sulfated-zirconia has been studied for the isomerization of *n*-butane to isobutane, a hydrocarbon used in the production of oxygenates and alkylates.

_____

*Corresponding author. Tel.: +1-608-262-1095; fax: +1-608-262-5434.

[1]Current address: Air Products and Chemicals, Inc., 7201 Hamilton Boulevard, Allentown, PA 18195-1501, USA.

Many studies have been contributed to the understanding of sulfated-zirconia catalysts, and several authoritative reviews of this catalyst system have been compiled [1–7]. In this review, we focus on an analysis of the reaction kinetic behavior for butane conversion over sulfated-zirconia catalysts. In particular, we will examine various factors influencing catalyst activity, selectivity, and deactivation. We will also discuss reaction schemes, including initiation, propagation, and termination steps, of butane isomerization over sulfated-zirconia. This review is organized according to the following aspects:

(a) effects of preparation methods on catalyst performance;
(b) catalyst deactivation during butane isomerization;
(c) surface acidity and its role in butane isomerization;
(d) effect of catalyst hydration state on catalyst performance;
(e) surface chain reactions; and
(f) feasibility of redox processes.

2. Effects of preparation methods on catalyst performance

Sulfated-zirconia catalysts can be produced via several methods. Yamaguchi [3] prepared sulfated metal oxides by adding SO_2, SO_3 or H_2S to a metal oxide containing oxygen vacancies and, subsequently, oxidizing the adduct to form sulfated species. Hattori et al. [8], Hochmann et al. [9], Arata et al. [10], Hsu et al. [11], Tanabe et al. [2], and Thorat et al. [12] reported that one can obtain sulfated-zirconia by adding $(NH_4)_2SO_4$ or H_2SO_4 directly to the metal oxide (usually in its hydroxylated form) and then calcining the sample in air or oxygen. The preparation and characterization of sulfated-zirconia catalysts have been reviewed by Davis et al. [5], and Song et al. [6].

Tanabe et al. [2], Arata et al. [10], Nascimiento et al. [13], Davis et al. [5], Chen et al. [14], Babou et al. [15], and Morterra et al. [16] have indicated that various factors, such as preparation method, sulfate loading, activation temperature, and moisture content of the catalyst, are important in determining the activity of sulfated-zirconia catalysts. For example, studies by

Corma et al. [17], Arata et al. [10], Clearfield et al. [18], and Yamaguchi [3] showed that the calcination temperature affects the activity of the catalyst for hydrocarbon isomerization. Hino and Arata [19] observed maxima near 850–950 K in plots of activity vs. calcination temperature for sulfated-zirconia catalysts prepared by different procedures. Low activity was seen for catalysts calcined at temperatures <773 K or >1073 K.

The activity for isomerization of butane was found to be related to the crystallographic phase of the sulfated-zirconia catalyst. Tanabe et al. [2] found that, as a consequence of calcination in air or oxygen between 773 and 923 K, the crystallographic phase of the catalyst transforms from amorphous to tetragonal. Navío et al. [20] found that calcination of this catalyst at higher temperatures causes a further change to a monoclinic phase, as well as a concomitant reduction in catalytic activity. The active catalysts showed tetragonal X-ray patterns. Guo et al. [21] reported similar behavior for the dependence on calcination temperature of catalytic activity and the crystallographic phase of sulfated-zirconia catalysts. For samples calcined at temperatures >1073 K, the changes observed in the XRD peak intensities of zirconia and sulfated-zirconia catalysts indicated a transformation in the crystallographic phase from tetragonal to monoclinic. Corma et al. [17] considered that the presence of a tetragonal phase in sulfated-zirconia could be correlated to catalytic activity for isomerization. Apparently, the tetragonal phase of zirconia is metastable, and Tanabe et al. [2] proposed that sulfation seems to stabilize both, the tetragonal phase and the specific surface area at lower temperatures. The sulfur content of the sulfated-zirconia catalyst depends on calcination temperature and, in turn, affects the activity for n-butane isomerization. Chen et al. [14] reported a correlation between the rate of n-butane isomerization and the sulfur contents of sulfated-zirconia catalysts, together with the calcination temperature. Furthermore, a decrease in the specific surface area was noted for samples subjected to higher calcination temperatures. Ward et al. [22] observed that, for samples treated at higher temperatures, higher sulfate loadings retarded the transformation from tetragonal to monoclinic. Li et al. [23] utilized UV Raman spectroscopy to characterize the surface phase of sulfated-zirconia during catalyst deactivation and

found a reconstruction from tetragonal to monoclinic phase.

Nascimiento et al. [13] also observed maxima in plots of catalytic activity vs. calcination temperature for sulfated-zirconia catalysts. Furthermore, a relationship was established between the sulfur content of the catalyst and the ratio of Brønsted-to-Lewis acid centers, as determined from pyridine adsorption measurements. At low sulfur content, Lewis acid sites predominate. However, as the sulfur content increases, the ratio of Brønsted-to-Lewis acid centers increases until the ratio exceeds unity. In addition, a maximum in the activity of the catalyst for isomerization was noted for equal numbers of Brønsted and Lewis sites. The relative numbers of Lewis and Brønsted acid centers are dependent on the sulfate loading and the calcination temperature. Nascimiento et al. [13] and Morterra et al. [16] reported that a minimum sulfate loading of 1% (w/w) S is necessary for Brønsted acidity to occur.

3. Catalyst deactivation during butane isomerization

3.1. Deactivation behavior

Sulfated-zirconia catalysts undergo deactivation during isomerization of n-butane and isobutane. We have found that a simple first-order deactivation model (i.e. $-dr_{iso}/dt = k_{deact} \times r_{iso}$, where r_{iso} is the isomerization rate and k_{deact} a deactivation constant) is useful to compare the deactivation behavior during the isomerization of n-butane and isobutane over sulfated-zirconia under various conditions. This first-order deactivation behavior gives rise to linear semi-log plots of the isomerization rate vs. reaction time, as exhibited by most of the kinetics data in butane isomerization over sulfated-zirconia catalysts (see Figs. 1–3) [24]. For example, this linear relationship is exhibited for isobutane isomerization over the entire reaction period (see Fig. 2). This linear relationship also exists for n-butane isomerization over sulfated-zirconia after 3 min time-on-stream (see Fig. 1). The following equation is, therefore, used to evaluate the catalyst deactivation constant during butane isomerization,

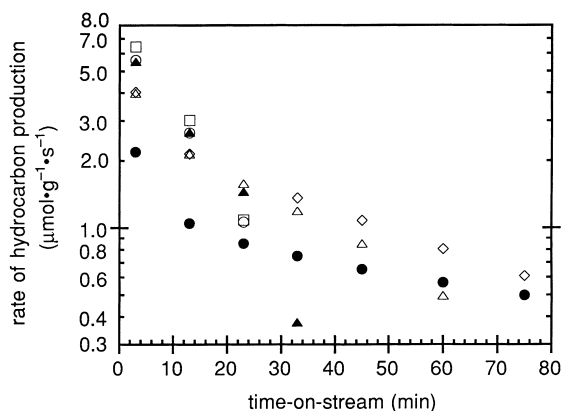$$r_{iso} = e^{-k_{deact}(t-t_0)} \tag{1}$$

Fig. 1. Rates of hydrocarbon production vs. time-on-stream for isomerization of n-butane at 423 K over sulfated-zirconia dried at 588 K for (●) 10%, (◇) 23%, (△) 36%, (▲) 67%, (□) 83%, (○) 100%, n-butane (containing olefin impurities) in the feed. (modified from Ref. [24]).

where t is the reaction time and t_0 the time after which the data follow first-order deactivation kinetics. Our kinetics studies [24,25] showed that the rate of catalyst deactivation increases as the concentration of n-butane (containing olefin impurities in the feed) increases for n-butane isomerization over sulfated-zirconia, together with an increase in the initial rate of hydrocarbon production at 3 min time-on-stream. For example, k_{deact} (after 3 min time-on-stream) increases from ∼0.02 min^{-1} at 10% n-butane to ∼0.15 min^{-1} at
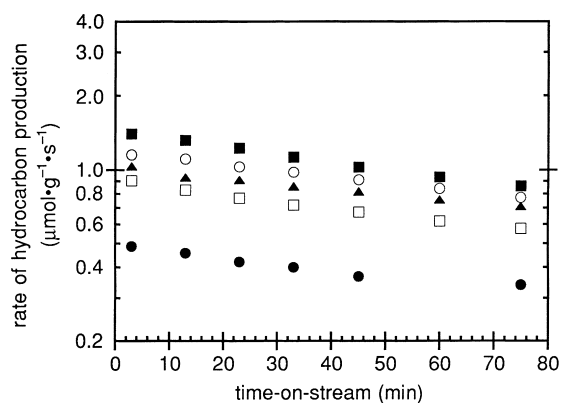

Fig. 2. Rates of hydrocarbon production vs. time-on-stream for isomerization of isobutane at 423 K over sulfated-zirconia dried at 588 K for (●) 10%, (□) 25%, (○) 53%, (▲) 77%, (■) 100%, isobutane (containing olefin impurities) in the feed. (modified from Ref. [24]).
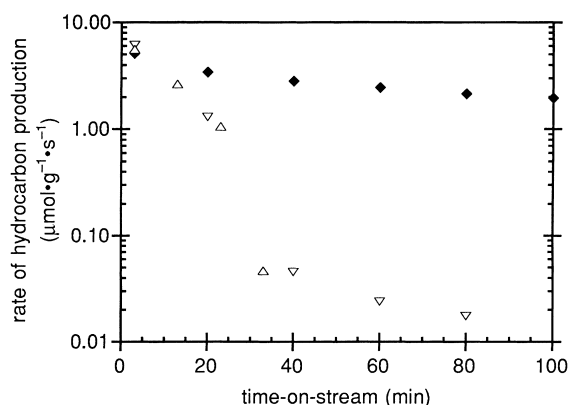
Fig. 3. Rates of hydrocarbon production vs. time-on-stream for isomerization of *n*-butane at 423 K over sulfated-zirconia dried at 588 K for 100% *n*-butane feed for which the C_4-olefins were retained ($\triangledown$, ∼1200 ppm), ($\triangle$, ∼100 ppm), and removed (<1 ppm) via ($\blacklozenge$) an olefin trap (activated H-mordenite held at 298 K). (modified from Ref. [24]).

100% *n*-butane (see Fig. 1). However, for isobutane isomerization over sulfated-zirconia, the values of k_{deact} are ∼0.006 min^{-1} for all concentrations of isobutane (containing olefin impurities in the feed) over the entire reaction time (see Fig. 2). This comparison of the deactivation behavior between the isomerization of *n*-butane and isobutane shows that the rate constant for deactivation is significantly smaller during isobutane isomerization than during *n*-butane isomerization over sulfated-zirconia catalysts.

The foregoing deactivation behavior suggests that a major cause of catalyst deactivation under our experimental conditions is related to the presence of *n*-butane or impurities, particularly olefins, within the *n*-butane feed stream. In this respect, we [24] also examined the effect of olefinic impurities on the rate of catalyst deactivation by using an olefin trap (H-mordenite) to remove olefins from the feed stream (to levels lower than 1 ppm). We observed that removal of olefins from the feed decreases the deactivation constant for *n*-butane isomerization over sulfated-zirconia. For example, the value of k_{deact} for a 100% *n*-butane feed decreases from ∼0.15 min^{-1} in the presence of feed olefins to ∼0.007 min^{-1} in the absence of feed olefins (see Fig. 3), and similar results are observed for a 10% *n*-butane feed. Importantly, we observed that the deactivation constant is similar for 10% and 100% *n*-butane feeds in the absence of

olefinic impurities [24]. By contrast, for isobutane isomerization over sulfated-zirconia, the deactivation constant is essentially the same, ∼0.006 min^{-1}, with, and without, the presence of feed olefins for both, 10% and 100% isobutane feeds [24]. Therefore, the presence of feed olefins increases the deactivation rate during *n*-butane isomerization but does not affect the deactivation behavior during isobutane isomerization.

3.2. Origins for deactivation of sulfated-zirconia catalysts

Garin et al. [26], Comelli et al. [27], Cheung et al. [28], and Chen et al. [14] suggested that an important cause for deactivation for sulfated-zirconia catalysts is the formation of coke at the active sites. Spielbauer et al. [29] detected allylic and polyenylic species during *n*-butane isomerization over sulfated-zirconia in the absence of hydrogen. Although the nature of coke formation is unclear, highly dehydrogenated carbonaceous species are considered to be precursors for coke formation. During isomerization of *n*-butane, straight chain C_4 species (butane and primarily butene species) are able to undergo dehydrogenation to form dienes, which may subsequently lead to formation of coke. However, during isomerization of isobutane, branched C_4 species cannot form conjugated carbon–carbon double bonds and, thus, cannot form the highly dehydrogenated precursors to coke. Therefore, the rate of catalyst deactivation is slower during isobutane isomerization than during *n*-butane isomerization. According to the foregoing argument, we consider that coke formation may be primarily responsible for the rapid deactivation of sulfated-zirconia catalysts during *n*-butane isomerization, and also be responsible for the faster deactivation during *n*-butane isomerization than during isobutane isomerization.

It appears that *n*-C_4 olefins are the primary species responsible for deactivation during *n*-butane isomerization, since the value of the deactivation constant increases when the concentration of olefins increases in the *n*-butane feed (associated with the increase of *n*-butane concentration). This consideration also explains the observation that the deactivation constants are similar for 10% and 100% *n*-butane feeds for which the olefinic impurities have been removed [24].

In addition to differences in the rates of coke formation during n-butane isomerization vs. isobutane isomerization, it is also important to address differences in the rates of removal of coke precursor species. In this respect, isobutane may act as a better hydride transfer agent than n-butane [30,31], thereby preventing the accumulation of carbonaceous species on the catalyst surface which may be precursors to coke formation. During isomerization of n-butane and isobutane, olefinic species may be converted by oligomerization processes to higher molecular weight species, and these species may be converted by hydride transfer with butane to higher molecular alkanes [32]. Indeed, higher molecular weight alkanes, e.g. C_6-species, were observed in the reactor effluent and, more importantly, higher rates of production of C_6-species were observed during isobutane isomerization than during n-butane isomerization [32]. When olefins were present in the feed, the rate of production of C_6-species during n-butane isomerization decreased to non-detectable levels within 30 min, while the rate of production of C_6-species during isobutane isomerization was constant with time. In addition, we [24] found that sulfated-zirconia could continue to convert feed olefins during isobutane isomerization even when the catalyst exhibited low catalytic activity for isomerization. In contrast, feed olefins were initially converted during n-butane isomerization; however, olefins were eventually detected in the effluent and their appearance coincided with a decrease in the catalytic activity exhibited by the catalyst for n-butane isomerization. Thus, removal of higher molecular weight species through hydride transfer with isobutane or n-butane is responsible for the long-term conversion of feed olefins, and this process may decrease the rate of coke formation from these higher molecular-weight precursor species.

We [24] also observed that the rate of catalyst deactivation during isobutane isomerization is negligible over H-mordenite at low levels of feed olefins, whereas sulfated-zirconia catalysts show slow, but measurable, deactivation under these conditions. This slow deactivation of sulfated-zirconia may be related to slow reduction of the catalyst, as suggested by Yori et al. [33] and Ng et al. [34]. In this respect, the oxidation ability of the sulfate group over sulfated-zirconia is considered to be an important function in initiating the reaction by generating reactive carbonaceous species during butane isomerization [26,35–49]. Therefore, irreversible reduction of surface sulfate groups may also cause deactivation of the catalyst. Indeed, Ng et al. [34] observed the production of hydrogen sulfide in the effluent stream during n-butane isomerization over sulfated-zirconia catalysts.

3.3. Isobutane isomerization as a probe reaction

As presented above, we found that isobutane isomerization shows slower deactivation than n-butane isomerization over sulfated-zirconia [24]. Therefore, isobutane isomerization can be used as an effective probe reaction to study the catalytic properties of sulfated-zirconia at conditions for which pseudo-steady state kinetic data can be collected. In addition, isobutane isomerization is a useful probe reaction to study reaction schemes for butane isomerization over solid acid catalysts, since the complications that result from deactivation by coke formation can be neglected. With this probe reaction, we developed a kinetic model for isobutane isomerization over H-mordenite at pseudo-steady state reaction conditions [50], a case where the acid sites control catalyst performance. We then extended this analysis to study the reaction kinetics of isobutane isomerization over sulfated-zirconia catalysts [51].

4. Surface acidity and its role in butane isomerization

4.1. Characteristic of surface acidity

In view of the unique properties of sulfated-zirconia for butane isomerization, Arata and Hino [19] suggested that these materials might be superacidic. However, more recent studies of the acid strength of sulfated-zirconia catalysts by various research groups [46,52–58] indicate that these materials exhibit acid strengths similar to those displayed by strong solid acids, for example H–Y zeolite. Moreover, assignment of superacidity based on observed catalytic activity may not be appropriate. For example, Sachtler et al. [46] found that, while sulfated-zirconia promoted with Fe and Mn exhibited similar acid strength as unpromoted sulfated-zirconia, the promoted catalyst displayed higher catalytic activity

for butane isomerization. In addition, Gates et al. [59,60] determined that the presumed superacidity of promoted sulfated-zirconia did not extend to high-temperature cracking reactions, and they suggested that low-temperature isomerization may not be solely catalyzed by acid sites.

Nevertheless, surface acidity plays an important role in butane isomerization over sulfated-zirconia catalysts. Many studies have been devoted to understanding the nature of the acidity of sulfated-zirconia catalysts, as discussed in various reviews [1–7]; in particular, the recent reviews by Song and Sayari [6] and by Sachtler et al. [7], and the related references therein. In general, the distribution of acid types has typically been investigated using infrared studies of adsorbed pyridine for sulfated-zirconia. Morterra et al. [16,61–64] found mostly Lewis acid sites on sulfated-zirconia samples, although the authors also noted the possible existence of Brønsted acidity for samples prepared under certain conditions (e.g. high sulfate loadings) [16]. Furthermore, Morterra et al. [62] suggested that the presence of Lewis acid sites was vital for high isomerization activity, but they did not exclude possible contributions from Brønsted acid sites. Yamaguchi et al. [65] found that catalysts evacuated at 773 K displayed only Lewis acid sites, and Jin et al. [66] also stated that their sulfated-zirconia samples possessed only Lewis acidity. However, most reports currently agree as to the presence of Brønsted acidity (as well as Lewis acidity), especially for samples with high sulfate loadings.

Lunsford et al. [67] used ^{31}P-NMR spectroscopy to probe the nature of Lewis and Brønsted acid sites on sulfated-zirconia catalysts. These authors found evidence for the existence of both, Lewis and Brønsted acidity and suggested that Brønsted acid sites were needed for high catalytic activity. Waqif et al. [68] also found Lewis and Brønsted acidity on sulfated-zirconia and suggested that the increase in the number of Brønsted acid sites from hydration came at the expense of the Lewis acid sites. Nascimento et al. [13] proposed that Brønsted and Lewis acid sites must both be present on the catalyst surface to generate superacidic properties. Chen et al. [14] proposed that both, strong Lewis and Brønsted acid sites are needed for n-butane isomerization. Riemer et al. [69] observed Brønsted acidity for a sulfated-zirconia catalyst calcined at 873 K which was active for the

isomerization of n-butane. In addition, Lewis acid centers were observed for this material via infrared spectroscopy of adsorbed carbon monoxide. Arata et al. [10], Sohn and Kim [70], Guo et al. [21], Ebitani et al. [71], Clearfield et al. [18] and Hino and Arata et al. [19] all observed both, Lewis and Brønsted acid sites on various sulfated-zirconia samples. Davis et al. [5] summarized the results of various investigators and concluded that probably Brønsted acidity exists on sulfated-zirconia catalysts.

4.2. Microcalorimetric characterization of surface acidity

Microcalorimetric measurements of the adsorption of ammonia have been used effectively to probe the acidic properties of various metal oxides and zeolite catalysts [72–79]. We employed microcalorimetry to measure the heats of ammonia adsorption to determine the number and acid strength distribution of the acid sites on a sulfated-zirconia sample calcined at 848 K containing 1.8% (w/w) S. As shown in Fig. 4, we found that the differential heat of ammonia adsorption at 423 K decreases with increasing ammonia coverage, indicating a distribution of acid site strengths [55]. This catalyst contains ≈30 μmol/g of strong acid sites, having differential heats of NH_3 adsorption in the range of 150–165 kJ/mol, and 40 μmol/g of acid sites with intermediate strength, having similar differ-
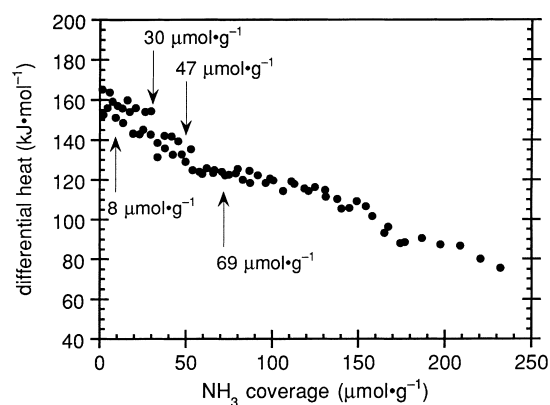

Fig. 4. Differential heat of NH_3 adsorption vs. adsorbate coverage at 423 K for a sulfated-zirconia sample calcined at 848 K in oxygen. The amounts of NH_3 used in the selective poisoning of acid sites over sulfated-zirconia were based on this result, as indicated in the plot. (modified from Ref. [55]).

ential heats of NH_3 adsorption in the range of 125–140 kJ/mol. A further plateau of acid sites can be distinguished at $\approx$120 kJ/mol, followed by a gradual decrease in the differential heat to a value of $\approx$70 kJ/mol with increasing ammonia coverage.

Jin et al. [66] found that the saturation ammonia coverage is ca. 260 μmol/g on a sulfated-zirconia sample prepared using ammonium sulfate. This value is similar to the total coverage of ammonia in our microcalorimetric study. Corma et al. [17,80] detected between 10 and 30 μmol/g of strong acid sites in ammonia TPD studies of sulfated-zirconia catalysts (corresponding to desorption at ca. 815 K), and this value is in agreement with the coverage found on our sulfated-zirconia sample for strong sites with differential heats of ammonia adsorption between 150 and 165 kJ/mol.

A combination of microcalorimetric and infrared spectroscopic studies of ammonia adsorption on our sulfated-zirconia catalyst indicated that the strong acid sites with differential heats near 150–165 kJ/mol consist of Brønsted and, possibly, Lewis acid centers, while sites with differential heats between 125 and 140 kJ/mol are mainly Brønsted acid centers [55]. In agreement with many other studies of surface acidity of sulfated-zirconia, as discussed in the foregoing, we conclude that the 70 μmol/g of active sites for n-butane isomerization with differential heats of NH_3 adsorption >125 kJ/mol exhibit mainly Brønsted acid sites and a smaller number of Lewis acid sites [55].

4.3. Selective poisoning of acid sites on sulfated-zirconia catalysts

To probe the relationship between acid-site strength and catalytic properties for n-butane isomerization, we [56] studied the kinetics of n-butane isomerization over sulfated-zirconia catalysts for which the acid sites of the catalysts were selectively poisoned with various amounts of adsorbed ammonia, based on the results of microcalorimetric studies [55]. Selective poisoning with adsorbed ammonia decreases the activity of the catalyst for n-butane isomerization, as shown in Fig. 5. The initial activity is reduced significantly when the first 8–15 μmol/g of strong acid sites are selectively poisoned with ammonia. However, the deactivation curves are still characterized by rapid initial deactivation followed by a region of slower
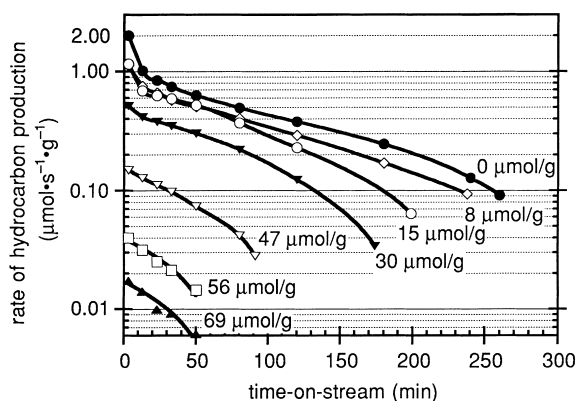

Fig. 5. Rates of hydrocarbon production vs. time-on-stream for n-butane isomerization at 423 K over sulfated-zirconia catalysts dried at 588 K, for which the acid sites were selectively poisoned by adsorbed NH_3 with (●) 0, (◇) 8, (○) 15, (▼) 30, (▽) 47, (□) 56, and (▲) 69 μmol g^{-1}. (modified from Ref. [56]).

deactivation that can be described by Eq. (1). Upon poisoning the first 30 μmol/g of strong acid sites with NH_3, the first regime of initial rapid deactivation is essentially eliminated. After poisoning with 47 μmol/g of ammonia, which corresponds to 8.4% of the total sulfur on the surface, the initial activity is an order of magnitude lower than that of the unpoisoned catalyst. Progressively larger NH_3 doses of 56 and 69 μmol/g lead to further decreases in catalytic activity. The selectivity to isobutane is ca. 93% for the unpoisoned catalyst. Similar isobutane selectivities have been reported for sulfated-zirconia catalysts by Yori et al. [33] at 573 K, Corma et al. [81] at 423 K, and Chen et al. [14] at 473, 523, and 573 K. The main side-products observed include propane, isopentane, and n-pentane. Some C_6 species were also observed in small amounts. The addition of up to 30 μmol/g of NH_3 leads to slight decreases in the isobutane selectivity. The selectivity to isobutane becomes as low as 74% for the catalyst that was poisoned with 69 μmol/g of NH_3.

Selective poisoning experiments provide further insight into the effects of acid strength on the activity and deactivation of the catalytic sites. Experiments, where 8, 15, or 30 μmol/g of ammonia were dosed onto the catalyst (see Fig. 5), indicate that the high initial activity and rapid deactivation of the catalyst seem to be related to the strongest 25 μmol/g of acid sites (differential heats of ammonia adsorption

of 145–165 kJ/mol). As mentioned earlier, whereas some of these sites may be Lewis acid sites, most are Brønsted acid sites [55]. The kinetics measurements over the sulfated-zirconia catalyst selectively poisoned with 30 and 47 µmol/g of ammonia show that, although acid sites with heats of 125–145 kJ/mol do not show initial high activity, these sites contribute to long-term catalytic activity. Selective poisoning with 56 and 69 µmol/g of ammonia shows that weaker acid sites (heats of 120–125 kJ/mol) have low catalytic activities. Selectivity to isobutane is less affected by the acid strength of the active sites than is the catalytic activity. Significant reductions in isobutane selectivity were observed only after the strong acid sites have been poisoned by ammonia at a level of 47 µmol/g.

5. Effect of hydration state on catalyst performance

5.1. Hydration state of sulfated-zirconia catalysts

Sulfated-zirconia catalysts are complicated by the fact that their performance is sensitive to the catalyst treatment conditions [1,3,5,13,14,16,20,22,67,80,82–84]. For example, Morterra et al. [16], Babou et al. [53], Zhang et al. [83], Escalona Platero et al. [85], Arata [1] and Norman et al. [84] showed that the temperature at which the catalyst is dried after calcination and exposure to atmospheric moisture is important in determining catalytic activity. Arata [1] reported that, for a catalyst calcined at 923 K, a maximum in isomerization activity is attained after drying the sample at 623 K. Babou et al. [15,53] have suggested that the surface sites on sulfated-zirconia may need small quantities of water to be active, and they proposed that a combination of Brønsted acid sites and surface-bound water is needed for catalytic activity. Arata and Hino [10], studying the benzylation of toluene over a sulfated alumina catalyst, observed a maximum in activity when the catalyst was dried at 563 K. On the other hand, Morterra et al. [63,64] and Keogh et al. [86] have shown that water poisons the active sites. In addition, Morterra et al. [16], Arata [1], Babou et al. [53], Lunsford et al. [67], Comelli et al. [27], and Zhang et al. [83] have found in spectroscopic studies of adsorbed basic probe molecules that water
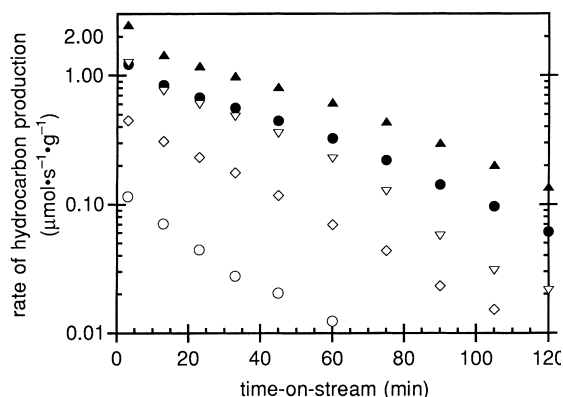

Fig. 6. Rates of hydrocarbon production vs. time-on-stream for *n*-butane isomerization at 423 K over sulfated-zirconia catalysts dried at (●) 473, (▲) 548, (▽) 623, (◇) 673, and (○) 773 K. (modified from Ref. [87]).

transforms Lewis acid sites of sulfated-zirconia into Brønsted acid sites.

5.2. Performance of sulfated-zirconia catalysts for butane isomerization

We used reaction kinetics studies of butane isomerization and water adsorption/desorption experiments to examine the effects of water on the catalytic activity of sulfated-zirconia catalysts [87]. First, we found that initial activity for *n*-butane isomerization changes with the drying temperature of the catalyst, as shown in Fig. 6. Second, for a catalyst dried at 773 K, the initial activity is a function of the amount of water added to the dehydrated sample. Specifically, adding small quantities of water to the dried catalyst leads to a marked increase in catalytic activity, and maximum activity appears to occur at ca. 75 µmol g^{-1}, while continuous addition of excess amount of water (>75 µmol g^{-1}) starts to decrease the catalytic activity [87].

We examined the reversibility of the rehydration process and found out that structural or chemical changes may take place at temperatures >723 K that cannot be restored by full rehydration of the catalyst at 423 K, unless the drying occurs in an oxidizing environment [87]. Essentially, our studies indicated that the effects on catalytic activity caused during the drying process can be reversed by addition of water at 423 K under certain conditions. Accordingly, the effects of

drying at progressively higher temperatures are most probably caused by the removal of water from the catalyst.

Infrared spectroscopic studies of the sulfated-zirconia catalyst suggest that the removal of water, upon drying from 588 to 773 K, does not significantly alter the concentration of Brønsted acid sites on the catalyst used in our study [57,58]. This result suggests that the decrease in catalytic activity, observed experimentally for a sulfated-zirconia catalyst dried at 773 K compared to a catalyst dried at 588 K, is not related to conversion of Brønsted acid sites to Lewis acid sites.

In addition, the results of ammonia poisoning experiments discussed above [55,56] show that a sulfated-zirconia catalyst dried at 423 K has ca. 70 µmol/g of active acid sites, while our hydration studies show that ca. 75 µmol/g of water are needed to promote a sulfated-zirconia catalyst dried at 773 K. This similarity between the numbers of acid sites and water-adsorption sites suggests that these sites may be related.

5.3. Promotion of n-butane isomerization by hydroxyl groups

On a dehydrated sulfated-zirconia catalyst (drying at 773 K), the initial heat of adsorption of water is ≈205 kJ/mol, although sites are discernible that display various strengths of interaction with the surface [57,58]. The heat of adsorption of water is higher than that of ammonia, at least for the first 100 µmol/g of adsorbed species [57,58]. Since water is a weaker base than ammonia, the high differential heat of adsorption suggests that water dissociates on the surface, for example, by interacting with bridging oxygen atoms to form new hydroxyl groups on the surface [88,89]. These higher heats are typical for dissociative adsorption of water to form surface hydroxyl groups [57,58,88–90]. This conclusion is consistent with the higher concentration of hydroxyl groups on sulfated-zirconia samples dried at lower temperatures [58].

Essentially identical heats of adsorption were measured for the adsorption of water on zirconia and on sulfated-zirconia, which suggests that water adsorbs on the zirconia support rather than on the sulfate or acid sites for our adsorption conditions [91]. In addi-

tion, we have shown that surface rehydration does not alter the number nor the strength of the acid sites, and addition of water to a dehydrated catalyst did not convert Lewis acid sites to Brønsted sites, as revealed by microcalorimetric and infrared spectroscopic measurements of ammonia adsorption [57,58]. These results suggest that rehydration does not alter the acid character of the catalyst, instead it serves to promote the existing acid sites. Thus, our studies indicate that the active sites for butane isomerization require an optimum state of hydration as well as an acidic component.

Sulfated-zirconia catalysts that are active for *n*-butane isomerization contain non-acidic hydroxyl groups. As revealed by Adeeva et al. [46], Kustov et al. [54], Morterra et al. [62], and Escalona Platero et al. [85], broad IR absorbance in the region of 2800 to 3500 cm^{-1} indicates that surface OH groups form strong hydrogen bonds to each other or to other groups on the surface. This behavior also indicates that the surface of the catalyst dehydrated at 588 K is populated by hydroxyl groups that are removed by drying at 773 K.

The absence of a correlation between the heat of adsorption of ammonia and catalytic activity for the isomerization of *n*-butane over sulfated-zirconia [58] may suggest that this reaction is not strictly acid-catalyzed. This hypothesis has been proposed by Gates et al. [60], who compared the products of the reaction of *n*-butane over Fe- and Mn-promoted sulfated-zirconia with those formed over H-ZSM-5. The presence of acid sites is a necessary but not a sufficient condition for high catalytic activity for isomerization of *n*-butane at the given reaction conditions. In particular, this reaction over our sulfated-zirconia catalyst dried at 588 K is effectively eliminated after the strongest, 70 µmol/g, of acid sites have been neutralized with ammonia [56]; however, the catalyst dried at 773 K shows low activity even though it possesses strong acid sites.

6. Surface chain reaction

6.1. Reaction scheme

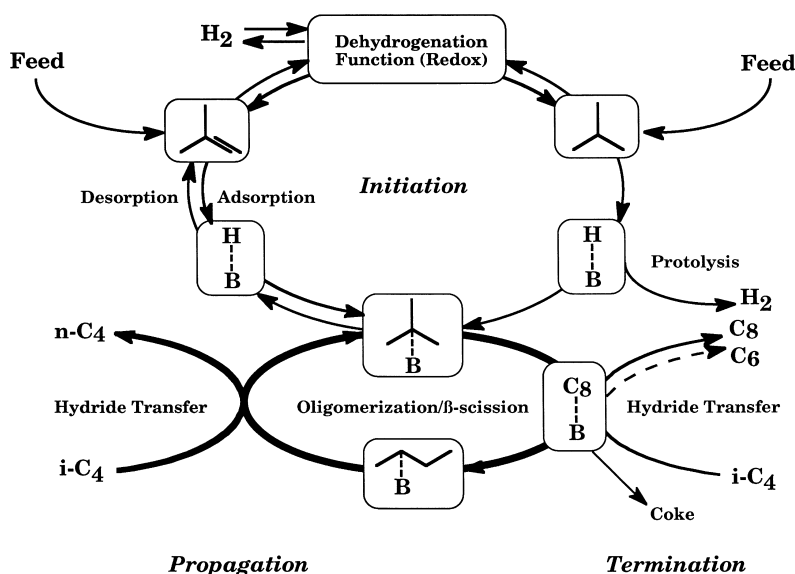Butane isomerization over sulfated-zirconia at 423 K can be viewed as a surface chain reaction

Fig. 7. Surface chain reaction scheme, comprising initiation, propagation, and termination steps, for isomerization of butane at ca. 420 K over sulfated-zirconia. (modified from Ref. [32]).

comprising initiation, propagation, and termination steps, as illustrated in the reaction scheme in Fig. 7. The surface chain reaction can be initiated via several pathways, for example adsorption of feed olefins onto acid sites, in situ generation of olefins from dehydrogenation processes of isobutane and subsequent adsorption of the olefins onto acid sites, or in situ generation of reactive intermediates via protolysis of isobutane by strong acid sites. There is general consensus that the propagation steps for butane isomerization at low temperatures are bi-molecular processes involving C_8 species [25,28,47,48,92–96]. The propagation steps involve oligomerization of C_4 species to form C_8 species, rearrangement and ß-scission of C_8 species, and hydride transfer from gas-phase isobutane to the reactive intermediates, leading to isomerization products and isobutyl reactive intermediates. The termination steps involve coke formation, as well as hydride transfer between isobutane and the higher molecular-weight reactive intermediates to form, for example, C_6 and C_8 alkanes. In this scheme, reactive species are represented as protonated species associated with their conjugate bases on the surface. The degree of charge distribution on the reactive intermediate is not specified here, for example whether the reactive intermediate is a carbenium ion (full charge

transfer), a neutral surface alkoxyl species, or a partially charged surface species.

In the propagation steps, the reactive intermediates undergo various processes, including oligomerization, ß-scission, and isomerization. Eventually, an *n*-butyl reactive intermediate is formed on the surface, which can undergo hydride transfer with isobutane to form gaseous *n*-butane and an isobutyl reactive intermediate. The isobutyl reactive intermediate can then participate in further oligomerization, ß-scission, and isomerization steps. Other reaction products can be produced via alternate oligomerization-cleavage pathways and hydride transfer steps.

Fig. 8 outlines some of the oligomerization, ß-scission, and isomerization steps involved in these propagation steps during isobutane isomerization. Brouwer [30,31] has studied and classified the relative rates of cracking and isomerization processes for carbenium ions in superacid solutions. The oligomerization of isobutylene and an isobutyl reactive intermediate (Step I) results in a trimethylpentyl reactive intermediate (2,2,4-trimethylpentyl species). According to Brouwer [31], rapid equilibration takes place among the various trimethylpentyl isomers, and these alkyl shifts are designated as type A isomerizations. The 2,2,3-trimethylpentyl species can undergo ß-scis-
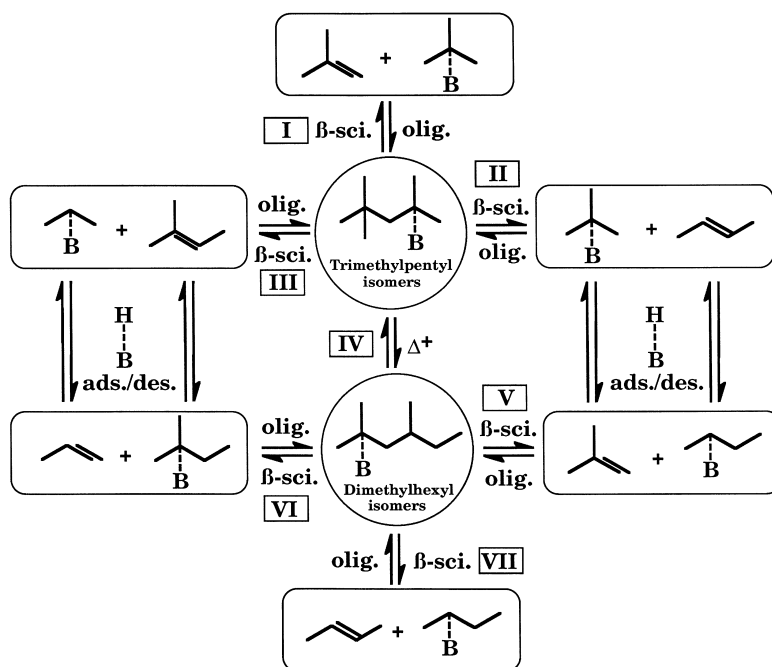
Fig. 8. Possible pathways in propagation steps for C_4 isomerization via C_8 intermediates. Notation: olig., oligomerization; ß-sci., ß-scission; Δ^+, cyclopropyl ring formation; ads./des., adsorption and desorption. (modified from Ref. [50]).

sion (Step II) to form an isobutyl reactive intermediate and gaseous *n*-butene. This cleavage, type B1 cracking, is from a secondary reactive intermediate to a tertiary species. Alternatively, the 2,3,4-trimethylpentyl isomer can undergo ß-scission (Step III) to form a propyl reactive intermediate and an isopentyl olefin. This cleavage, type B2 cracking, is from a tertiary reactive intermediate to a secondary species. Type A cracking, from a tertiary reactive intermediate to a tertiary species, involves cleavage of the 2,2,4-trimethylpentyl species (Step I) to form isobutylene and an isobutyl reactive intermediate. Type B isomerization, a branching rearrangement, can proceed from the trimethylpentyl species via a cyclopropyl intermediate to form the dimethylhexyl species (Step IV). Dimethylhexyl species can also undergo type A isomerization to give other dimethylhexyl isomers. The 2,4-dimethylhexyl species can undergo ß-scission (Step V) to form an *n*-butyl reactive intermediate and isobutylene, B2-type cracking. Alternatively, formation of the 3,3-dimethylhexyl isomer and ß-scission via B1 type cracking (Step VI) results in propylene and an isopentyl reactive intermediate. Type C crack-

ing, from a secondary reactive intermediate to a secondary species, involves cleavage of the 3,4-dimethylhexyl reactive intermediate (Step VII) to form *n*-butene and a *n*-butyl reactive intermediate. The relative rates of the aforementioned reactions are expected to follow the trend: Hydride shift > A isomerization > A cracking > B isomerization > B1, B2 cracking > C cracking. Since Martens et al. [97] have observed that the rate of A cracking can be faster than A isomerization for solid catalysts, the order of the relative rates of the different cracking and isomerization steps can change depending on the reaction conditions.

6.2. Propagation steps

Based on carbenium ion chemistry in solution, the isomerization of butane can proceed via two reaction pathways, that is mono-molecular and bi-molecular processes [26,46,92,98,99]. The mono-molecular mechanism involves the formation of a primary carbenium ion, which is energetically unfavorable compared to a secondary carbenium ion. In the

bi-molecular mechanism as proposed by Guisnet et al. [92,93], two C_4 species interact to form a C_8 intermediate, and the C_8 intermediate undergoes rearrangements and ß-scission to form isomerized C_4 species, or C_3 and C_5 species. Importantly, the bi-molecular mechanism does not proceed through a primary carbenium ion. With evidence from isotopic scrambling experiments, Sachtler et al. [47,48] showed that the bimolecular mechanism is the dominate reaction pathway for the isomerization of *n*-butane over Fe–Mn promoted sulfated-zirconia catalysts. Gates et al. [28,94,95] also suggested a bi-molecular pathway for *n*-butane and isobutane isomerization over Fe- and Mn- promoted sulfated-zirconia. In agreement with the bi-molecular mechanism, our reaction kinetics studies [25] suggested that the isomerization reaction pathway proceeds via a C_8 intermediate which can undergo isomerization and ß-scission to produce *n*-butane or isobutane as well as the observed disproportionation products (C_3 and C_5 species). Recently, Trung Tran et al. [96] suggested that dihydrogen inhibited the bi-molecular mechanism and higher temperatures favored the mono-molecular pathway. Finally, the propagation steps are completed by hydride transfer from isobutane to the *n*-butyl species formed via oligomerization/ß-scission steps to form *n*-butane and adsorbed isobutyl species. Sachtler et al. [7] recently reviewed studies of the propagation steps in the mechanism of *n*-butane isomerization.

6.3. Initiation steps

Initiation may occur via adsorption of olefins present in the feed stream onto acid sites. Sachtler et al. [48,49] proposed that the isomerization reaction is initiated by small amounts of olefins, either in the feed or produced by the catalyst. A decrease in the level of olefins fed to the catalyst resulted in lower catalytic activity accompanied by slower catalyst deactivation [24,25,49]. Tábora et al. [100] reported promotional effects of olefins on the catalytic activity for butane isomerization over promoted sulfated-zirconia.

Clearly, the presence of olefins in the feed affects the reaction behavior; however, it is still unclear whether the presence of olefins in the feed is required for catalytic activity over sulfated-zirconia. For example, Tábora et al. [101] reported that olefins in the feed are necessary for butane isomerization at low tem-
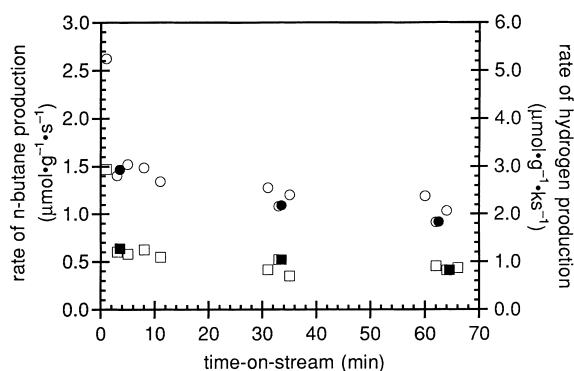

Fig. 9. Rates of dihydrogen production (open symbols) and *n*-butane production (filled symbols) vs. time-on-stream for isobutane isomerization at 423 K over sulfated-zirconia dried at 588 K (SZ-588) with 100% isobutane in feed. (●) *n*-Butane production over SZ-588, on left axis; (○) dihydrogen production over SZ-588, on right axis; (■) *n*-butane production over SZ-588 with 45 μmol/g of preadsorbed ammonia, on left axis; (□) dihydrogen production over SZ-588 with 45 μmol/g of preadsorbed ammonia, on right axis. (modified from Ref. [32]).

peratures over sulfated-zirconia catalysts dried at elevated temperatures. However, as shown in Fig. 3, and also in Fig. 9, for our pretreatment conditions of the sample, we have found that sulfated-zirconia is still active for butane isomerization at 423 K even without detectable levels of olefins present in the feed [24,25,32]. This observation suggests that sulfated-zirconia is able to generate reactive intermediates in situ to initiate the surface chain reaction.

One process to generate reactive intermediates involves in situ dehydrogenation of isobutane to form dihydrogen and isobutylene during isobutane isomerization over sulfated-zirconia catalyst. Isobutylene can then adsorb onto acid sites to form reactive intermediates. Liu et al. [49] have suggested that unpromoted sulfated-zirconia is able to produce butene from butane. Importantly, as shown in Fig. 9, we have detected evolution of dihydrogen during butane isomerization over sulfated-zirconia at 423 K in the absence of feed olefins [32]. It should be noted that C_4 olefins were not detected in the effluent during isobutane isomerization over sulfated-zirconia; therefore, olefins produced in the dehydrogenation cycle are consumed by the catalyst.

Fig. 9 shows the rates of dihydrogen production and *n*-butane production vs. time-on-stream for isobutane isomerization at 423 K over sulfated-zirconia dried at

588 K (SZ-588) and over SZ-588 with 45 µmol/g of preadsorbed ammonia. As seen in Fig. 9, the rate of dihydrogen evolution correlates with the rate of iso-butane isomerization. We also observed a similar correlation between the rate of dihydrogen evolution and the rate of isomerization of isobutane for isobu-tane isomerization over the sulfated-zirconia catalyst dried at 773 K (SZ-773). In our previous studies [57,58,87], it was observed that sulfated-zirconia, dried at 773 K, exhibits lower butane isomerization activity than sulfated-zirconia dried at 588 K. Accord-ingly, the rates of dihydrogen evolution and isobutane isomerization over the SZ-773 sample are both an order of magnitude lower than the corresponding rates over the SZ-588 sample.

Similar to isobutane isomerization, dihydrogen evo-lution was also detected during *n*-butane isomerization over sulfated-zirconia. The rate of dihydrogen produc-tion during *n*-butane isomerization is an order of magnitude lower than the rate of dihydrogen produc-tion during isobutane isomerization for 3–70 min time-on-stream.

The production of olefins by sulfated-zirconia may occur via a redox process. Farcasiu et al. [35–38] proposed that sulfated-zirconia is a bi-functional cat-alyst, which possesses both, strong acidity and oxida-tive properties. These authors suggested that alkane reactions over sulfated-zirconia might be initiated through a one-electron oxidation of the alkane by sulfate species to produce a carbonation precursor. Riemer et al. [39] suggested that sulfated-zirconia possesses oxidizing properties in addition to strong acidity, based on the detection of oxidized phosphor-ous species on the surface of sulfated-zirconia follow-ing exposure of the catalyst to trimethylphosphene. Ng et al. [34] suggested that sulfate species are reduced during *n*-butane isomerization over sulfated-zirconia by *n*-butane or by hydrogen generated in situ. Xu et al. [40] showed that sulfate groups are reduced on sul-fated-zirconia catalysts in the presence of dihydrogen. TPD studies by Okuhara et al. [41] and TPR studies by Dicko et al. [42] on sulfated-zirconia catalysts also indicated that sulfate groups can be reduced. TPD studies of benzene adsorbed on promoted sulfated-zirconia indicated the presence of oxidized species on the surface [43–45]. Adeeva et al. [46] detected the presence of sites capable of oxidizing acetonitrile on sulfated-zirconia and Fe- and Mn-promoted sulfated-
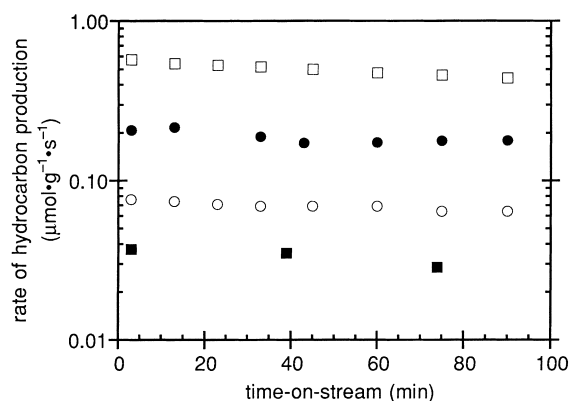

Fig. 10. Rate of hydrocarbon production vs. time-on-stream for isobutane isomerization at 423 K over sulfated-zirconia dried at 588 K with 10% isobutane (containing olefin impurities), and 0% (□), 15% (●), 50% (□), and 90% (■) H_2, and the balance helium.

zirconia. Sachtler et al. [47–49], Garin et al. [26], and Wan et al. [43] proposed that the promotional effects of the addition of Pt or Fe–Mn to sulfated-zirconia may be related to the dehydrogenation activity of the additive.

As reported by Liu et al. [49], and Hosoi et al. [102], the presence of dihydrogen in the feed decreases the rate of butane isomerization over sulfated-zirconia. Fig. 10 shows this suppression effect of feed dihydro-gen for the rate of hydrocarbon production during isobutane isomerization over sulfated-zirconia. For example, while the initial rate of hydrocarbon produc-tion is ∼0.6 µmol g^{-1} s^{-1} in the absence of feed hydrogen, the initial rate decreases from ∼0.2 to ∼0.04 µmol g^{-1} s^{-1} when the concentration of feed H_2 increases from 15% to 90%. It is important to note that H_2 affects the reaction kinetics differently on sulfated-zirconia than on H-mordenite. As shown elsewhere [50], the presence of H_2 in the feed has no effect on the catalytic activity for isobutane iso-merization over H-mordenite for our reaction condi-tions. In addition, chemisorption measurements for dihydrogen on sulfated-zirconia at 423 K showed no detectable uptake. Therefore, this suppression of butane isomerization by dihydrogen is not caused by the competitive adsorption of hydrogen on the acid sites, that is dihydrogen does not block the acid sites. Rather, it appears that dihydrogen in the feed may inhibit isomerization by shifting the equilibrium for

butane dehydrogenation, thereby limiting the rate of initiation.

In contrast to a redox process, it is possible to form olefins via protolysis of isobutane. Gates et al. [103] proposed that initiation processes over sulfated-zirconia-based catalysts occur when the alkane is protonated by an acid site, forming a carbonium ion species (or transition state) which decomposes to generate a reactive hydrocarbon intermediate (i.e. a protonated olefin associated with the conjugate base form of the acid site) and dihydrogen or methane. As proposed previously by Olah [104], this reaction pathway requires extremely strong acidity. However, results from recent studies suggest that sulfated-zirconia catalysts exhibit acid strength similar to strong solid acids, for example H-mordenite, which are not generally considered to be superacidic [46,52–58]. Furthermore, in the absence of feed olefins, H-mordenite is not active for isobutane isomerization at 473 K [50]. Therefore, it appears that isobutane at low temperatures cannot be activated via protolysis by an acid site on H-mordenite or by an acid site with acid strength similar to H-mordenite. Furthermore, selective poisoning of the strongest acid sites on sulfated-zirconia with ammonia does not eliminate catalytic activity (see Fig. 9) [32], although the rates of hydrocarbon production and dihydrogen production are suppressed. In particular, dihydrogen evolution was still observed even though the strongest acid sites of sulfated-zirconia were poisoned by preadsorbed ammonia. This result suggests that protonation of isobutane by the strongest acid sites is not the primary mode for initiation of isobutane isomerization.

6.4. Termination steps

As noted earlier, termination of the surface chain reaction may occur via coke formation and by hydride transfer from isobutane to higher molecular weight species on the catalyst. In this respect, we have observed production of higher molecular weight paraffins, for example C_6 paraffins, during isobutane isomerization and n-butane isomerization [24]. We observed that the rates of production of these higher molecular-weight paraffins during isobutane isomerization are higher than during n-butane isomerization [24]. Furthermore, when C_4 olefins were present in the

feed during isobutane isomerization, no C_4 olefins were detected in the effluent. It appears that during isobutane isomerization, sulfated-zirconia can effectively consume feed olefins via oligomerization processes to form higher molecular-weight species followed by hydride transfer from isobutane to produce higher molecular-weight paraffins. In contrast to this situation for isobutane isomerization, C_4 olefins were eventually detected in the reactor effluent when C_4 olefins were present in the feed during n-butane isomerization [24]. According to Brouwer [30,31], hydride abstraction from isobutane is more favorable than hydride abstraction from n-butane. Thus, sulfated-zirconia does not consume feed olefins as effectively during n-butane isomerization as during isobutane isomerization, mostly likely because of slower hydride transfer from n-butane to the higher molecular-weight species on the catalyst surface.

We can estimate the chain length of the isomerization reaction by dividing the rate of hydrocarbon production by the rate of dihydrogen evolution. For isobutane isomerization, the chain length is ca. 500, that is 500 propagation cycles occur for every isobutylene species produced by initiation. Chain lengths of 10–20 were observed by Tábora et al. [100]; however, these chain lengths were measured by injecting olefins into the reactor, and the higher olefin concentrations achieved in these experiments may lead to side reactions which would decrease the chain length. Also, it appears that the drying temperature employed during catalyst pretreatment affects the rates of both dihydrogen and hydrocarbon production, as discussed above. Thus, the observation by Davis et al. [101], olefins in the feed are necessary for butane isomerization over sulfated-zirconia at low temperatures might be caused by slower rates of initiation on a more dehydroxylated surface (i.e. 773 K drying) and by lower rates of hydride transfer by n-butane than by isobutane.

7. Feasibility of redox processes

To understand the nature of the initiation steps, we employed density functional theory to study the feasibility of dehydrogenation processes over sulfated-zirconia [32]. Density functional theory (DFT) methods have proven to be useful to predict accurate
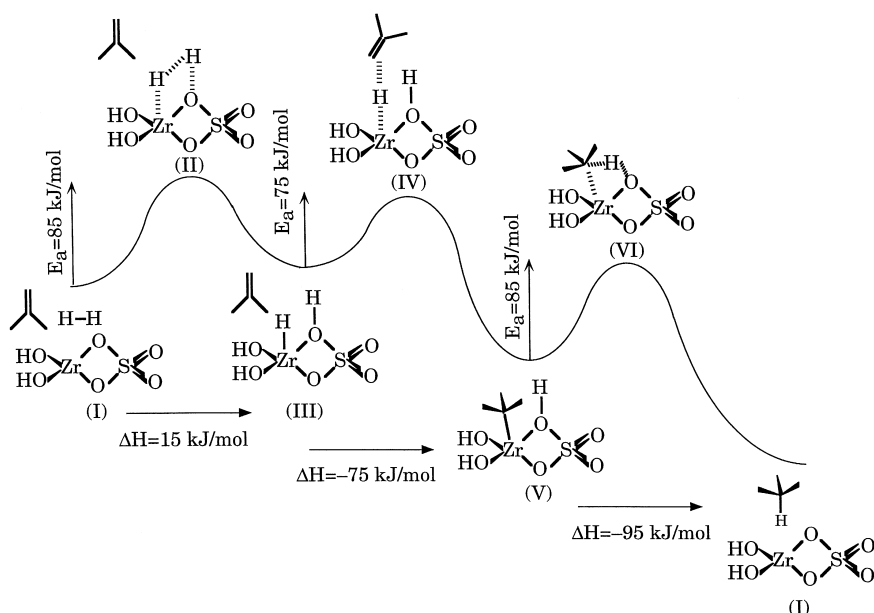
Fig. 11. Energy profile of a possible reaction pathway for dihydrogen dissociation and isobutylene hydrogenation over the sulfated-zirconia cluster.

geometries. Various models for the structure of sulfate groups on sulfated-zirconia have been proposed in the literature [1,18,46,54,66,69,105,106]. These models were reviewed recently by Song and Sayari [6]. In our study [32], a representative structural model of sulfated-zirconia, similar to the model proposed by Arata [1] is used in the quantum-chemical calculations. As a feasibility study of the chemistry involved in the initiation process, a simplified representative structural model of sulfated-zirconia was used in quantum-chemical calculations, as shown in structure I of Fig. 11. In this sulfated-zirconia cluster, the sulfate group is connected to the zirconium atom via two bridging oxygen atoms. The two coordinating oxygen atoms are terminated by hydrogen atoms, in the form of hydroxyl groups, to maintain electrical neutrality for the entire cluster. The structure of this sulfated-zirconia cluster is similar to the model proposed by Tanabe et al. [2], and Yamaguchi [3]. This model was chosen to represent the S–O–Zr site and sulfate group which are the main features of numerous sulfated-zirconia models proposed. However, it should be noted that this model is only a simplified representative structure and it is used only for feasibility studies of possible initiation processes.

Fig. 11 shows the calculated results of the energy profile of a possible reaction pathway for dihydrogen dissociation and isobutylene hydrogenation over the sulfated-zirconia cluster. Structural parameters were determined by optimizing to stationary points on the potential energy surface using internal coordinates. The clusters resulting from optimization were classified as local minima or transition states on the energy surface by calculating the Hessian matrix numerically. For local minima, the eigenvalues of the Hessian matrix were all positive, whereas for transition states only one eigenvalue was negative. For these transition states, displacement along the eigenvector for the negative eigenvalue led to the reactant and product of the elementary step. As shown in Fig. 11, dihydrogen dissociation proceeds via a transition state (structure II) in which H–H interacts with the Zr–O site, to form a Zr–H bond and an O–H bond (structure III) over the sulfated-zirconia cluster. The calculated activation energy is ca. 85 kJ/mol for dihydrogen dissociation via this reaction pathway, and the calculated energy change associated with this mode of dihydrogen dissociation on the sulfated-zirconia cluster is ca. 15 kJ/mol. When isobutylene interacts with the dissociated hydrogen atoms on the sulfated-zirconia

cluster, calculations show that this process proceeds through a transition state (structure IV) in which the methylene group of isobutylene attacks the hydrogen atom bonded to zirconium. This transition state leads to the formation of an isobutyl species bonded to the zirconium atom (structure V). The calculated activation energy of this process is ca. 75 kJ/mol, and the calculated energy change associated with this mode of isobutylene adsorption is ca. −75 kJ/mol. The adsorbed isobutyl species combines with the hydrogen atom bonded to the neighboring bridging oxygen to form isobutane. The hydrogen atom associated with the bridging oxygen interacts with the tertiary carbon in the isobutyl species, passing through a transition state (structure VI) with an activation energy of ca. 85 kJ/mol. This transition state leads to the formation and subsequent desorption of isobutane, and the associated energy change is ca. −95 kJ/mol.
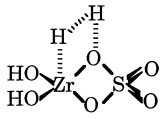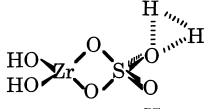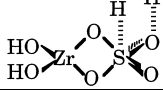
Other possible reaction pathways of dihydrogen dissociation over this sulfated-zirconia cluster were also examined, for example dihydrogen activation over the S=O site in the sulfate group. The calculated activation energies of the transition states for various modes of dihydrogen adsorption on the sulfated-zirconia cluster are listed in Table 1. As shown in Table 1, the activation energies for dihydrogen dissociation are much higher for interactions with S=O site compared to the aforementioned Zr–O site. These high activation energies of dihydrogen dissociation over S=O site suggest that the activation of dihydrogen

or isobutane over the Zr–O site is the most feasible pathway for dissociative adsorption.

Fig. 11 shows the reaction pathway of H$_2$ dissociation and isobutylene hydrogenation over a representative sulfated-zirconia cluster. According to our quantum-chemical calculations, H$_2$ may dissociate over the Zr–O site, and the activation energy of this step (ca. 85 kJ/ml) suggests that this process is feasible at our reaction conditions. Domen et al. [107,108] reported that H$_2$ dissociates heterolytically on ZrO$_2$ at room temperature, giving IR-active bands at 3668 and 1562 cm^{-1} from O–H and Zr–H stretching modes, respectively. Though other types of H$_2$ adsorption are also possible, for example associative adsorption and homolytic dissociative adsorption, the predominant form of H$_2$ adsorption on ZrO$_2$ at temperatures >223 K is heterolytic dissociative adsorption. The activation energy for this mode of adsorption was estimated to be ca. 40 kJ/mol from infrared spectroscopic measurements, and this result is in general agreement with our calculations. Moreover, theoretical studies of H$_2$ dissociative adsorption on a ZrO$_2$ surface by Nakatsuji et al. [109] showed that the calculated activation energy for heterolytic dissociation of H$_2$ was ca. 90 kJ/mol, and the heat of dissociative adsorption was exothermic by ca. 95 kJ/mol relative to gaseous H$_2$. Our results give an activation energy for H$_2$ dissociative adsorption over the sulfated-zirconia cluster similar to the value calculated by Nakatsuji et al. [109] for H$_2$ dissociative adsorption over zirconia. The adsorption heats were different from these calculations, probably because of different clusters used in the calculations.

Based on our calculations, one possible pathway for isobutylene hydrogenation is that isobutylene may interact with the hydrogen atom bonded to zirconium to form an isobutyl species associated with zirconium, and this isobutyl species may further combine with a hydrogen atom attached to neighboring oxygen to form isobutane. Our calculated activation energies are ca. 75 kJ/mol for the first step and ca. 85 kJ/mol for the second step, suggesting that this reaction pathway is feasible at our reaction conditions. This pathway implies that isobutylene hydrogenation may proceed over a Zr–O site. A similar reaction pathway was proposed by Kokes et al. [110] for ethylene hydrogenation over zinc oxide, where H$_2$ dissociative adsorption is activated over a Zn–O site to form Zn–H

Table 1
Activation energies of various modes of dihydrogen dissociation over the sulfated-zirconia cluster

Interaction Site for dihydrogen dissociation	Structural model of transition state	Activation energy (kJ/mol)
Zr–O		85
O in S=O		315
S=O		285

and O–H species with an activation energy even lower than that over a Zr–O site. Domen et al. [111] reported that ethylene did not react with preadsorbed ZrH and ZrOH species at temperatures ∼223 K. However, this reaction temperature is much lower than our reaction temperature (423 K).

Following the reverse direction of Fig. 11, isobutane may undergo dissociative adsorption over a Zr–O site to form an isobutyl species associated with Zr and an H species associated with the neighboring bridging oxygen atom. The isobutyl species may participate in initiation reactions of the acid-catalyzed butane isomerization over sulfated-zirconia by desorbing from Zr to form isobutylene and ZrH, or by migrating onto acid sites to form reactive intermediates in the acid-catalyzed surface chain reaction. The hydrogen atoms in the forms of Zr–H and O–H may combine to form dihydrogen molecules. It should be noted that isobutylene was not detected during the isobutane isomerization over sulfated-zirconia catalysts. This observation suggests that isobutylene, once formed, undergoes further reactions, for example reactions involved in initiation of the surface chain reaction, and in oligomerization.

We have shown in earlier works that the rate of butane isomerization over sulfated-zirconia catalysts is sensitive to the hydration state of the catalyst [57,58,87]. González et al. [57,58] showed that the catalytic activity of sulfated-zirconia catalysts, dried at 773 K, could be increased by addition of ca. 70 µmol/g of water, and infrared spectra of this catalyst showed that the primary effect of this water addition was to increase the extent of hydrogen bonding on the surface. Thus, it is possible that the promotional effect is related to stabilization of the reactive intermediates by hydrogen bonding with the hydroxyl groups. The stabilization from hydrogen bonding may also facilitate the surface migration of isobutyl species from zirconium atoms to acid sites, thereby increasing the rate of isobutane dehydrogenation. Indeed, we observed a higher rate of dihydrogen production during isobutane isomerization over SZ-588 than over SZ-773.

In short, based on our quantum-chemical studies, a possible reaction pathway for dihydrogen dissociation, isobutylene hydrogenation, and isobutane dissociation over the sulfated-zirconia cluster is proposed, and the calculated activation energies suggest that this pathway is feasible at reaction conditions employed for butane isomerization (e.g., 423 K). These reactions may take place over the Zr–O site in the sulfated-zirconia cluster. The dehydrogenation of isobutane may be responsible for initiation process during butane isomerization over sulfated-zirconia, whereas dihydrogen dissociative adsorption and hydrogenation of isobutylene may be responsible for the inhibiting effect of H_2 on the rate of isomerization over sulfated-zirconia catalysts. It appears that the sulfate group does not participate directly in the initiation process of isobutane activation. However, the acid sites created by the sulfate groups on the catalyst are primarily responsible for the propagation steps in the surface chain reaction.

8. Conclusions

Sulfated-zirconia catalysts, prepared from zirconia modified with sulfuric acid or other sulfur-containing reagent, are active for the isomerization of butane at low temperatures, for example in the 300–423 K range. Factors, such as the preparation method, sulfate loading, activation temperature, and moisture content of the catalysts, are important in determining the activity of the sulfated-zirconia catalysts. A maxima in catalytic activity at temperatures near 850–950 K for catalyst calcination was observed for sulfated-zirconia catalysts. The sulfur content of the catalyst also depends on catalyst calcination temperatures and, in turn, affects the activity for *n*-butane isomerization.

Sulfated-zirconia catalysts undergo rapid deactivation during isomerization of *n*-butane when olefins are present in the feed. Removal of the olefinic impurities present in the feed via an olefin trap decreases the rate of catalyst deactivation during *n*-butane isomerization over sulfated-zirconia. The rates of deactivation during isobutane isomerization over sulfated-zirconia catalysts are much slower, even in the presence of feed olefins, than those during *n*-butane isomerization. Rapid deactivation of these catalysts during isomerization of *n*-butane appears to be caused primarily by coke formation, resulting from dehydrogenation of straight chain olefinic species that are present in the *n*-butane feed or that are produced on the catalyst under reaction conditions. Higher rates of production of higher molecular-weight species (e.g. C_6-species)

were observed during isobutane isomerization rather than during *n*-butane isomerization. It appears that more effective hydride transfer of surface species during isobutane isomerization, rather than during *n*-butane isomerization, may remove coke precursors. On account of slow deactivation, isobutane isomerization may be an effective probe reaction to study solid acid catalysts at pseudo-steady state reaction conditions for which effects of catalyst deactivation are insignificant.

Sulfated-zirconia catalysts exhibit strong, but not super, acidity, with acid strength similar to strong solid acids, for example H–Y zeolite. Microcalorimetry and infrared spectroscopic studies of ammonia adsorption showed that there are ca. 70 μmol g^{-1} of acid sites with adsorption heat between 125 and 165 kJ/mol, and these acid sites are mainly of the Brønsted type. Kinetic studies using selective poisoning of acid sites over sulfated-zirconia with adsorbed ammonia showed that these acid sites are responsible for the high catalytic activity. In addition to catalyst acidity, the hydration state of the catalysts also affects the catalytic activity significantly. The initial catalytic activity changes with the drying temperature for sulfated-zirconia, and the activity is a function of the amount of water added to the dehydrated catalyst. An amount of 75 μmol g^{-1} of water was needed to promote the dehydrated catalyst to maximum initial activity. Dehydration of the catalyst at either 588 K or 773 K did not alter the heat or the extent of ammonia adsorption, as well as the type of acid sites, that is Brønsted acid sites. The promotion effect of water may have resulted from hydroxyl groups generated during drying treatments or water dissociative adsorption.

Butane isomerization at 423 K over sulfated-zirconia can be viewed as being a surface chain reaction comprising initiation, propagation, and termination steps. The surface chain reaction can be initiated, for example, by adsorption of olefins present in the feed stream onto acid sites to form protonated species associated with the conjugate base form of the acid sites. Importantly, sulfated-zirconia is active for butane isomerization at 423 K without olefins present in the feed, indicating that sulfated-zirconia is able to generate olefins in situ to initiate the surface chain reaction. These olefins can be generated on sulfated-zirconia by dehydrogenation of butanes over redox

sites or by protolysis of butanes over strong acid sites. Experimental evidence for the generation of olefins by sulfated-zirconia catalysts was provided by detecting the production of dihydrogen during butane isomerization. Although the activation of isobutane over sulfated-zirconia may proceed via protolysis on strong acid sites, dihydrogen evolution during isobutane isomerization was still observed over sulfated-zirconia catalysts that have been selectively poisoned by preadsorbed ammonia. Thus, protolysis of isobutane by strong acid sites does not appear to be the primary mode for initiation for butane isomerization over sulfated-zirconia. Instead, it appears that the dehydrogenation of butane over sulfated-zirconia takes place via a redox process. Quantum-chemical calculations, employing the density-functional theory, suggest that the dissociative adsorption of dihydrogen, isobutylene hydrogenation, and dissociative adsorption of isobutane are feasible over the sulfated-zirconia cluster, and these reactions take place over Zr–O sites.

Acknowledgements

References

[1] K. Arata, Adv. Catal. 37 (1990) 165.
[2] K. Tanabe, H. Hattori, T. Yamaguchi, Crit. Rev. Surf. Chem. 1 (1990) 1.
[3] T. Yamaguchi, Appl. Catal. 61 (1990) 1.
[4] A. Corma, Chem. Rev. 95 (1995) 559.
[5] B.H. Davis, R.A. Keogh, R. Srinivasan, Catal. Today 20 (1994) 219.
[6] X. Song, A. Sayari, Catal. Rev. – Sic. Eng. 38 (1996) 329.
[7] V. Adeeva, H.Y. Liu, B.Q. Xu, W.M.H. Sachtler, Topics in Catal., 1998, in press.
[8] H. Hattori, O. Takahashi, M. Takagi, J. Tanabe, J. Catal. 68 (1981) 132.
[9] T. Hochmann, K. Setínek, Collect. Czech. Chem. Commun. 56 (1991) 1404.

[10] K. Arata, M. Hino, N. Yamagata, Bull. Chem. Soc. Jpn. 63 (1990) 244.

[11] C.Y. Hsu, C.R. Heimbuch, C.T. Armes, B.C. Gates, Chem. Commun., 1992, pp. 1645.

[12] T.S. Thorat, V. Yadav, G. Yadav, Appl. Catal. A: Gen. 90 (1992) 73.

[13] P. Nascimiento, C. Akratopoulou, M. Oszagyan, G. Courdurier, C. Travers, J.F. Joly, J.C. Vedrine, New Frontiers in Catalysis, Elsevier, Amsterdam, 1993, pp. 1185.

[14] F.R. Chen, G. Courdurier, J. Joly, J.C. Vedrine, J. Catal. 143 (1993) 616.

[15] F. Babou, B. Bigot, P. Sauset, J. Phys. Chem. 97 (1993) 11501.

[16] C. Morterra, G. Cerrato, V. Bolis, Catal. Today 17 (1993) 505.

[17] A. Corma, M.I. Juan-Rajadell, J.M. López-Nieto, A. Martínez, C. Martínez, Appl. Catal. A: Gen. 111 (1994) 175.

[18] A. Clearfield, G.P.D. Serrette, A.H. Khazi-Syed, Catal. Today 20 (1994) 295.

[19] M. Hino and K. Arata, Chem. Commun. (1980) 851.

[20] J.A. Navío, M. Macías, C. Real, G. Colón, Mater. Lett. 20 (1994) 345.

[21] C. Guo, S. Yao, J. Cao, Z. Qian, Appl. Catal. A: Gen. 107 (1994) 229.

[22] D.A. Ward, E.I. Ko, J. Catal. 150 (1994) 18.

[23] C. Li, P.C. Stair, Catal. Lett. 36 (1996) 119.

[24] K.B. Fogash, Z. Hong, J.M. Kobe, J.A. Dumesic, Appl. Catal. 172 (1998) 107.

[25] K.B. Fogash, R.B. Larson, M.R. Gonzalez, J.M. Kobe, J.A. Dumesic, J. Catal. 163 (1996) 138.

[26] F. Garin, D. Andriamasinoro, A. Abdulsamad, J. Sommer, J. Catal. 131 (1991) 199.

[27] R.A. Comelli, C.R. Vera, J.M. Parera, J. Catal. 151 (1995) 96.

[28] T.K. Cheung, J.L. d'Itri, B.C. Gates, J. Catal. 151 (1995) 464.

[29] D. Spielbauer, G.A.H. Mekhemer, E. Bosch, H. Knözinger, Catal. Lett. 36 (1996) 59.

[30] D.M. Brouwer, H. Hogeveen, in A.J. Streitwieser, R.W. Taft (Eds.), Progress in Physical Organic Chemistry, John Wiley & Sons, New York, vol. 9, 1972, pp. 179.

[31] D.M. Brouwer, in R. Prins, G.C.A. Schuit (Eds.), Chemistry and Chemical Engineering of Catalytic Processes, Sijthoff and Noordhoff, Alphen a/d Rijn, vol. 137, 1980.

[32] Z. Hong, K.B. Fogash, R.M. Watwe, B. Kim, B.I. Masqueda-Jimenez, M.A. Natal-Santiago, J.M. Hill, J.A. Dumesic, J. Catal. 178 (1998) 489.

[33] J.C. Yori, J.C. Luy, J.M. Parera, Appl. Catal. 46 (1989) 103.

[34] F.T.T. Ng, N. Horvát, Appl. Catal. A: Gen. 123 (1995) L197.

[35] D. Farcasiu, 214th National Meeting, Am. Chem. Soc., Las Vegas, NV, September 1997, pp. 745.

[36] D. Farcasiu, A. Ghenciu, G. Miller, J. Catal. 134 (1992) 118.

[37] D. Farcasiu, A. Ghenciu, J.Q. Li, J. Catal. 158 (1996) 116.

[38] D. Farcasiu, A. Ghenciu, Progr. NMR Spectro. 29 (1996) 129.

[39] T. Riemer, H. Knözinger, J. Phys. Chem. 100 (1996) 6739.

[40] B.Q. Xu, W.M.H. Sachtler, J. Catal. 167 (1997) 224.

[41] T. Okuhara, T. Nishimura, H. Watanabe, M. Misono, J. Mol. Catal. 74 (1992) 247.

[42] A. Dicko, X. Song, A. Adnot, A. Sayari, J. Catal. 150 (1994) 254.

[43] K.T. Wan, C.B. Khouw, M.E. Davis, J. Catal. 158 (1996) 311.

[44] A. Jatia, C. Chang, J.D. MacLeod, T. Okubo, M.E. Davis, Catal. Lett. 25 (1994) 21.

[45] E.C. Sikabwe, M.A. Coelho, D.E. Resasco, R.L. White, Catal. Lett. 34 (1995) 25.

[46] V. Adeeva, J.W. de Haan, J. Jänchen, G.D. Lei, V. Schünemann, L.J.M. van de Ven, W.M.H. Sachtler, R.A. van Santen, J. Catal. 151 (1995) 364.

[47] V. Adeeva, G.D. Lei, W.M.H. Sachtler, Appl. Catal. A 118 (1994) L11.

[48] V. Adeeva, G.D. Lei, W.M.H. Sachtler, Catal. Lett. 33 (1995) 135.

[49] H. Liu, V. Adeeva, G.D. Lei, W.M.H. Sachtler, J. Mol. Catal. A: Chem. 100 (1995) 35.

[50] K.B. Fogash, Z. Hong, J.A. Dumesic, J. Catal. 173 (1998) 519.

[51] K.B. Fogash, Z. Hong, J.A. Dumesic, Catal. Lett., 1998, in press.

[52] B. Umansky, J. Engelhardt, W.K. Hall, J. Catal. 127 (1991) 128.

[53] F. Babou, G. Courdurier, J.C. Vedrine, J. Catal. 152 (1995) 341.

[54] L.M. Kustov, V.B. Kazansky, F. Figueras, D. Tichit, J. Catal. 150 (1994) 143.

[55] K.B. Fogash, G. Yaluris, M.R. González, P. Ouraipryvan, D.A. Ward, E.I. Ko, J.A. Dumesic, Catal. Lett. 32 (1995) 241.

[56] G. Yaluris, R.B. Larson, J.M. Kobe, M.R. González, K.B. Fogash, J.A. Dumesic, J. Catal. 158 (1996) 336.

[57] M.R. González, J.M. Kobe, K.B. Fogash, J.A. Dumesic, J. Catal. 160 (1996) 290.

[58] M.R. González, K.B. Fogash, J.M. Kobe, J.A. Dumesic, Catal. Today 33 (1997) 303.

[59] T. Cheung, J.L. d'Itri, F.C. Lange, B.C. Gates, Catal. Lett. 31 (1995) 153.

[60] T.K. Cheung, J.L. d'Itri, B.C. Gates, J. Catal. 153 (1995) 344.

[61] F. Pinna, M. Signoretto, G. Strukul, G. Cerrato, C. Morterra, Catal. Lett. 26 (1994) 339.

[62] C. Morterra, G. Cerrato, F. Pinna, M. Signoretto, J. Phys. Chem. 98 (1994) 12373.

[63] C. Morterra, G. Cerrato, F. Pinna, M. Signoretto, G. Strukul, J. Catal. 149 (1994) 181.

[64] C. Morterra, V. Bolis, G. Cerrato, G. Magnacca, Surf. Sci. 307 (1994) 1206.

[65] T. Yamaguchi, T. Jin, T. Ishida, K. Tanabe, Mater. Chem. Phys. 17 (1987) 3.

[66] T. Jin, T. Yamaguchi, K. Tanabe, J. Phys. Chem. 90 (1986) 4794.

[67] J.H. Lunsford, H. Sang, S.M. Campbell, C. Liang, R.G. Anthony, Catal. Lett. 27 (1994) 305.

[68] M. Waqif, J. Bachelier, O. Saur, J.C. Lavalley, J. Mol. Catal. 72 (1992) 127.

[69] T. Riemer, D. Spielbauer, M. Hunger, G.A.H. Mekhemer, H. Knözinger, Chem. Commun. (1994) 1181.

[70] J.R. Sohn, H.W. Kim, J. Mol. Catal. 52 (1989) 379.

[71] K. Ebitani, J. Tsuji, H. Hattori, H. Kita, J. Catal. 135 (1992) 609.

[72] N. Cardona-Martínez, J.A. Dumesic, Adv. Catal. 38 (1992) 149.

[73] N. Cardona-Martínez, J.A. Dumesic, J. Catal. 128 (1991) 23.

[74] A. Auroux, A. Gervasini, J. Phys. Chem. 94 (1990) 6371.

[75] A. Auroux, M. Muscas, D.J. Coster, J.J. Fripiat, Catal. Lett. 28 (1994) 179.

[76] B.E. Spiewak, B.E. Handy, S.B. Sharma, J.A. Dumesic, Catal. Lett. 23 (1994) 207.

[77] D.J. Parrillo, C. Lee, R.J. Gorte, D. White, W.E. Farneth, J. Phys. Chem. 99 (1995) 8745.

[78] D.J. Parrillo, R.J. Gorte, W.E. Farneth, J. Am. Chem. Soc. 115 (1993) 12441.

[79] P. Carniti, A. Gervasini, A. Auroux, J. Catal. 150 (1994) 174.

[80] A. Corma, A. Martínez, C. Martínez, J. Catal. 149 (1994) 52.

[81] A. Corma, V. Fornés, M.I. Juan-Rajadell, J.M. López Nieto, Appl. Catal. A 116 (1994) 151.

[82] K. Mukaida, T. Miyoshi, T. Satoh, in: K. Tanabe, H. Hattori, T. Yamaguchi, T. Tanaka (Eds.), Acid–Base Catalysis, vol. 363, Kodansha, Tokyo, 1989.

[83] C. Zhang, R. Miranda, B.H. Davis, Catal. Lett. 29 (1994) 349.

[84] C.J. Norman, P.A. Goulding, I. McAlpine, Catal. Today 20 (1994) 313.

[85] E. Escalona Platero, M. Penarroya Mentruit, Catal. Lett. 30 (1995) 31.

[86] R.A. Keogh, R. Srinivasan, B.H. Davis, J. Catal. 151 (1995) 292.

[87] J.M. Kobe, M.R. González, K.B. Fogash, J.A. Dumesic, J. Catal. 164 (1996) 459.

[88] D.J. Coster, J.J. Fripiat, M. Muscas, A. Auroux, Langmuir 11 (1995) 2615.

[89] B.V. Romanovskii, K.V. Topchieva, L.V. Stolyarova, A.M. Alekseev, Kinetika Kataliz 11 (1969) 1525.

[90] B. Fubini, V. Bolis, M. Bailes, F.S. Stone, Solid State Ionics, 32/33 (1989) 258.

[91] K.B. Fogash, Ph.D. Dissertation, University of Wisconsin–Madison, 1997.

[92] C. Bearez, F. Avendano, F. Chevalier, M. Guisnet, Bull. Soc. Chim. France (1985) 346.

[93] M.R. Guisnet, Acc. Chem. Res. 23 (1990) 392.

[94] A.S. Zarkalis, C.Y. Hsu, B.C. Gates, Catal. Lett. 37 (1996) 1.

[95] A.S. Zarkalis, C.Y. Hsu, B.C. Gates, Catal. Lett. 29 (1994) 235.

[96] M. Trung Tran, N.S. Gnep, M. Guisnet, P. Nascimiento, Catal. Lett. 47 (1997) 57.

[97] J.A. Martens, P.A. Jacobs, J. Weitkamp, Appl. Catal. 20 (1986) 239.

[98] C. Bearez, F. Chevalier, M. Guisnet, React. Kinet. Catal. Lett. 22 (1983) 405.

[99] F. Garin, L. Seyfried, P. Girard, G. Maire, A. Abdulsamad, J. Sommer, J. Catal. 151 (1995) 26.

[100] J.E. Tábora, R.J. Davis, J. Catal. 162 (1996) 125.

[101] J.E. Tábora, R.J. Davis, J. Am. Chem. Soc. 118 (1996) 12240.

[102] T. Hosoi, T. Shimidzu, S. Itoh, S. Baba, H. Takaoka, T. Imai, N. Yokoyama, Prepr. Am. Chem. Soc. Div. Pet. Chem. 33 (1988) 562.

[103] T. Cheung, F.C. Lange, B.C. Gates, Catal. Lett. 34 (1995) 351.

[104] G.A. Olah, A. Molnar, Hydrocarbon Chemistry, John Wiley & Sons, Inc., New York, 1995.

[105] M. Bensitel, O. Saur, J.C. Lavalley, B.A. Morrow, Mater. Chem. Phys. 19 (1988) 147.

[106] R.L. White, E.C. Sikabwe, M.A. Coelho, D.E. Resasco, J. Catal. 157 (1995) 755.

[107] J. Kondo, Y. Skata, K. Domen, K. Maruya, T. Onishi, J. Chem. Soc., Faraday Trans. 86 (1990) 397.

[108] T. Onishi, H. Abe, K. Maruya, K. Domen, Chem. Commun. (1985) 617.

[109] H. Nakatsuji, M. Hada, H. Ogawa, K. Nagata, K. Domen, J. Phys. Chem. 98 (1994) 11840.

[110] R.J. Kokes, A.L. Dent, Adv. Catal. 22 (1972) 1.

[111] K. Domen, J. Kondo, K. Maruya, T. Onishi, Catal. Lett. 12 (1992) 127.